World Journal of Advanced Research and Reviews
eISSN: 2581-9615 CODEN (USA): WJARAI
Cross Ref DOI: 10.30574/wjarr
Journal homepage: https://wjarr.com/

(REVIEW ARTICLE)

Check for updates

Influence of the shape of the grain boundary on the I-V characteristic, power and diffusion capacity of the cylindrical grain solar cell

Modou Kara MBENGUE [1, 2, *], Serigne Ndiangue LEYE [2], Mamadou Salif DIALLO [2] and Senghane MBODJI [2]

[1] *Laboratory for Semiconductors and Solar Energy, Department of Physics, Faculty of Science and Technology, Cheikh Anta Diop University, Dakar, Senegal.*
[2] *Research team in Renewable Energies, Materials and Laser of the Department of Physics, Alioune DIOP University of Bambey, Bambey, Senegal.*

World Journal of Advanced Research and Reviews, 2025, 25(02), 858-870

Publication history: Received on 25 December 2024; revised on 04 February 2025; accepted on 07 February 2025

Article DOI: https://doi.org/10.30574/wjarr.2025.25.2.0361

Abstract

In this study, a numerical simulation of a three-dimensional model was carried out to analyze the excess minority carrier density in the base of a bifacial polycrystalline silicon solar cell composed of cylindrical grains. The solution obtained is adapted to boundary conditions that take into account the shape of the grain boundaries. The idea of the shape of the grain boundaries was used to characterize the charge carrier density of the solar cell illuminated from both sides and to evaluate the I-V characteristic, the power and the diffusion capacity. Plots of charge carrier density, power and diffusion capacity were used to investigate the influence of grain boundary shape on the electrical parameters of the n+-p-p+ solar cell. The results indicate that the grain boundary size plays a very significant role on the production activity of the solar cell. Therefore, this study highlights the importance of production losses in the cell due to the shape of the grain boundaries.

Keywords: Solar Cell; Cylindrical Grain; Grain Boundary; Polycrystalline; Numerical Resolution

1. Introduction

Improving the performance of photovoltaic solar cells requires quality control at all stages of solar cell manufacture [1]. Solar cell quality is highly dependent on microscopic and electrical parameters [2, 3]. The performance of the solar cell is governed by factors including the quality of the intra-grain material [4, 5], the surface finish and the properties of the grain boundaries [6, 7]. For these factors, the grain boundaries have a constraining contribution to the production, they participate in the decrease of the solar cell performance [8, 9].

In previous studies, the authors have developed numerous characterization methods in steady state, transient dynamic and frequency dynamic regimes with the aim of controlling the constraining parameters during cell manufacture [10, 11].

In this work, we propose a method for determining the equivalent electrical parameters associated with the shape of the grain boundaries in a bifacial solar cell composed of cylindrical grains under the static regime.

1.1. Theoretical study

The n^+-p polycrystalline solar cell is a device composed of small grains. The study of solar cells requires the adaptation of a grain model. This model can be spherical, cylindrical or columnar.

* Corresponding author: Modou Kara MBENGUE.

In this study, the work is oriented towards the cylindrical model shown in figure 1 below [12].

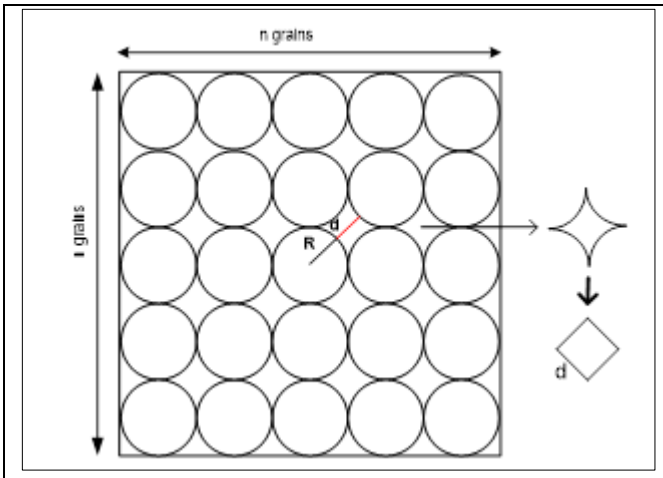

Figure 1 Schematic presentation in the (x, y) plane of a multicylindrical grain solar cell [12].

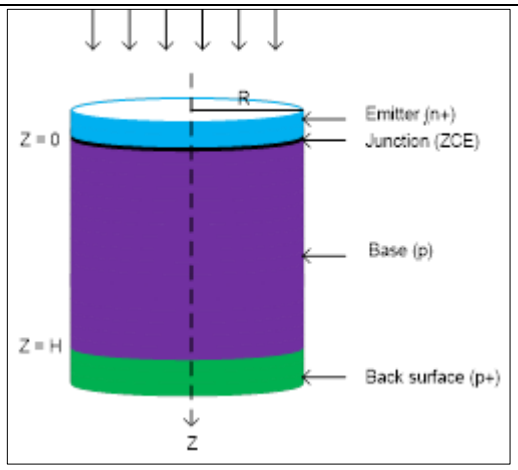

Figure 2 solar cell grain or crystal, simultaneous illumination [12].

1.1.1. We make the following assumptions

- The grains have a circular cross-section of radius R and their electrical properties are homogeneous;
- The solar cell also has grain boundaries of square cross-section and sizes whose values, d, vary from (0.0001 to 0.009 cm);
- Illumination is uniform, as that. The generation rate depends only on the depth in the z-base;
- The grain boundaries are perpendicular to the junction and their recombination rates are independent of the generation rate under illumination AM 1.5. The boundary conditions of the continuity equation are therefore linear;
- The contribution of the emitter and the space charge zone is neglected so that this analysis is only developed at the base of the photocell [13].

When the cell is illuminated with multispectral white light, the continuity equation for the excess minority charge carrier density photogenerated in the cell base can be written as follows [11]:

- Load or current distribution in cylindrical coordinates

$$\frac{\partial \delta(r,\theta,z,t)}{\partial t} + \vec{\nabla} \cdot \vec{J}(r,\theta,z,t) = 0 \quad (1)$$

- Load distribution for solar cells

$$\frac{\partial \delta(r,\theta,z,t)}{\partial t} = -\frac{1}{e}\vec{\nabla} \cdot \vec{J}(r,\theta,z,t) + G(z) - R(z) \quad (2)$$

$$G(z) = n \cdot a_i \cdot e^{-b_i \cdot z} \quad (3)$$

$$R(z) = \frac{\delta(r,\theta,z,t)}{\tau} \quad (4)$$

- Total cell current

$$\vec{J} = -eD\vec{\nabla}\delta(r,\theta,z,t) + e\mu\delta(r,\theta,z,t)\vec{E} \quad (5)$$

- Since we're working on the assumption of a quasi-neutral photopile base, we have:

$$\vec{E} = \vec{B} = \vec{0} \tag{6}$$

$$\vec{J} = -eD\vec{\nabla}\delta(r,\theta,z,t) \tag{7}$$

- In the static regime, charge carrier density is independent of time.

$$\frac{\partial\delta(r,\theta,z,t)}{\partial t} = 0 \tag{8}$$

Therefore:

$$-\frac{1}{e}\vec{\nabla}\cdot\vec{J}(r,\theta,z) + G(z) - R(z) = 0 \tag{9}$$

- Let's replace the expressions for J(r,θ,z) and R(z) in equation (9)

$$-\frac{1}{e}\vec{\nabla}\cdot(-eD\vec{\nabla}\delta(r,\theta,z)) + G(z) - \frac{\delta(r,\theta,z)}{\tau} = 0 \tag{10}$$

$$\vec{\nabla}\cdot\vec{\nabla}\delta(r,\theta,z) - \frac{\delta(r,\theta,z)}{D\cdot\tau} = -\frac{G(z)}{D} \tag{11}$$

$$\Delta\delta(r,\theta,z) - \frac{\delta(r,\theta,z)}{L^2} = -\frac{G(z)}{D} \tag{12}$$

- Laplacian in cylindrical coordinate

$$\Delta = \frac{\partial^2}{\partial r^2} + \frac{\partial^2}{\partial z^2} + \frac{1}{r^2}\frac{\partial^2}{\partial\theta^2} + \frac{1}{r}\frac{\partial}{\partial r} \tag{13}$$

$$\frac{\partial^2\delta(r,\theta,z)}{\partial r^2} + \frac{\partial^2\delta(r,\theta,z)}{\partial z^2} + \frac{1}{r^2}\frac{\partial^2\delta(r,\theta,z)}{\partial\theta^2} + \frac{1}{r}\frac{\partial\delta(r,\theta,z)}{\partial r} - \frac{\delta(r,\theta,z)}{L^2} = -\frac{G(z)}{D} \tag{14}$$

- By assumption, the electrical properties of the grains are homogeneous; this gives rise to cylindrical symmetry and in this case the angle θ is not taken into account. So the number of cylindrical coordinates is halved:

$$\frac{\partial^2\delta(r,z)}{\partial r^2} + \frac{\partial^2\delta(r,z)}{\partial z^2} + \frac{1}{r}\frac{\partial\delta(r,z)}{\partial r} - \frac{\delta(r,z)}{L^2} = -\frac{G(z)}{D} \tag{15}$$

- By analogy, diffusion in the grain boundary is modelled as follows:

$$\frac{\partial^2\delta(x,z)}{\partial x^2} + \frac{\partial^2\delta(x,z)}{\partial z^2} - \frac{\delta(x,z)}{L^2} = -\frac{G(z)}{D} \tag{16}$$

τ is the charge carrier lifetime, D and δ(x) are the diffusion coefficient, minority charge carrier density in the cell base, respectively;

$g(x)$ represents the rate of generation of the minority charge carrier density in the cell base and is written as [13]:

$$g(x) = \sum_{i=1}^{3} n \times a_i \times e^{b_i x} \quad (17)$$

a_i et b_i represent, the values of the AM1 spectrum ($cm^{-3}.s^{-1}$) and the silicon absorption coefficient (cm^{-1}), respectively.

The equations below represent the boundary conditions of the solar cell, with Sf representing the junction recombination rate, Sb the backside recombination rate and Sgb the grain boundary recombination rate [12, 14]:

For cylindrical grain

$$\left.\frac{\partial \delta(r,z)}{\partial z}\right|_{z=0} = \frac{Sf}{D}\delta(r, z=0) \quad (18)$$

$$\left.\frac{\partial \delta(r,z)}{\partial r}\right|_{r=R} = -\frac{Sgb}{D}\delta(r=R, z) \quad (19)$$

$$\left.\frac{\partial \delta(r,z)}{\partial z}\right|_{z=H} = -\frac{Sb}{D}\delta(r, z=H) \quad (20)$$

For the grain seal

$$\left.\frac{\partial \delta(x,z)}{\partial z}\right|_{z=0} = \frac{Sf}{D}\delta(x, z=0) \quad (21)$$

$$\left.\frac{\partial \delta(x,z)}{\partial x}\right|_{x=0} = -\frac{Sgb}{D}\delta(x=0, z) \quad (22)$$

$$\left.\frac{\partial \delta(x,z)}{\partial x}\right|_{x=d} = -\frac{Sgb}{D}\delta(x=d, z) \quad (23)$$

$$\left.\frac{\partial \delta(x,z)}{\partial z}\right|_{z=H} = -\frac{Sb}{D}\delta(x, z=H) \quad (24)$$

The inter-grain boundaries are characterized by a recombination velocity that is equal to $Sgb/2$. On the other hand, extra-grain boundaries, i.e. those formed by the first and last grains of the cell, have a recombination velocity which corresponds to Sgb. As a result, the solar cell production is the sum of the output that takes into account inter-grain boundaries and extra-grain boundaries.

1.2. Approximation of diffusion equations

1.2.1. Finite difference methods

This numerical solution involves transforming the continuous equation into an algebraic equation. To do this, an approximation $\delta_{i,j}$ of $\delta(r_i, z_j)$ must be found at certain points in r_i and z_j of the intervals [0, R] and [0, H] respectively.

We first divide these intervals into (n - 1) and (m - 1) sub-intervals (steps) of lengths $\Delta r = R/(n-1)$ and $\Delta z = H/(m-1)$ we note:

$$r_1 = 0 \qquad r_i = (i-1)\Delta r \qquad r_n = (n-1)\Delta r$$

$$z_1 = 0 \qquad z_j = (j-1)\Delta z \qquad z_m = (m-1)\Delta z$$

The boundary conditions are known and immediately obvious. All that remains is to determine:

$$\delta_{2,j},\ \delta_{3,j},\cdots\delta_{n-1,j} \text{ and } \delta_{i,2},\ \delta_{i,3},\cdots\delta_{i,m-1}$$

The solution strategy consists in replacing all the function's derivatives in the differential equation with finite-difference formulas at each point r_i and z_j for $i = 2,\cdots,n-1$ and $j = 2,\cdots,m-1$.

$$\frac{\partial^2\delta(r,z)}{\partial r^2} = \frac{\delta_{i-1,j} - 2\delta_{i,j} + \delta_{i+1,j}}{(\Delta r)^2} \tag{25}$$

$$\frac{\partial^2\delta(r,z)}{\partial z^2} = \frac{\delta_{i-1,j} - 2\delta_{i,j} + \delta_{i+1,j}}{(\Delta z)^2} \tag{26}$$

$$\frac{\partial^2\delta(r,z)}{\partial r^2} = \frac{\delta_{i+1,j} - \delta_{i,j}}{\Delta r} \tag{27}$$

$$\frac{\partial^2\delta(r,z)}{\partial x^2} = \frac{\delta_{i-1,j} - 2\delta_{i,j} + \delta_{i+1,j}}{(\Delta x)^2} \tag{28}$$

The continuity equations become:

$$\frac{\delta_{i-1,j} - 2\delta_{i,j} + \delta_{i+1,j}}{(\Delta r)^2} + \frac{\delta_{i,j-1} - 2\delta_{i,j} + \delta_{i,j+1}}{(\Delta z)^2} + \frac{1}{r_i}\frac{\delta_{i+1,j} - \delta_{i-1,j}}{\Delta r} - \frac{1}{L^2}\delta_{i,j} = -\frac{G_j}{D} \tag{29}$$

$$\frac{\delta_{i-1,j} - 2\delta_{i,j} + \delta_{i+1,j}}{(\Delta x)^2} + \frac{\delta_{i,j-1} - 2\delta_{i,j} + \delta_{i,j+1}}{(\Delta z)^2} - \frac{1}{L^2}\delta_{i,j} = -\frac{G_j}{D} \tag{30}$$

The boundary conditions:

$$\delta_{i,1} = \frac{D}{D + Sf\cdot\Delta r}\delta_{i,2} \tag{31}$$

$$\delta_{i,m} = \frac{D}{D + Sb\cdot\Delta r}\delta_{i,m-1} \tag{32}$$

$$\delta_{n,j} = \frac{D}{D + Sgb\cdot\Delta r}\delta_{n-1,j} \tag{33}$$

$$\delta_{1,j} = \frac{D}{D + Sgb \cdot \Delta x} \delta_{2,j} \quad (34)$$

$$\delta_{n,j} = \frac{D}{D + Sgb \cdot \Delta x} \delta_{n-1,j} \quad (35)$$

2. Results and discussion

2.1. Gap energy at the crystal interface

The gap energy at the crystal interface is given by the following relationship:

$$E_g = E_f + q\Phi + qV_d \quad (36)$$

- E_g represents the gap energy at the crystal interface
- E_f is the fermi energy
- V_d is the potential barrier
- $q\Phi$ is the output work

Figure 3 shows the evolution of the gap energy at the crystal interface as a function of grain boundary size.

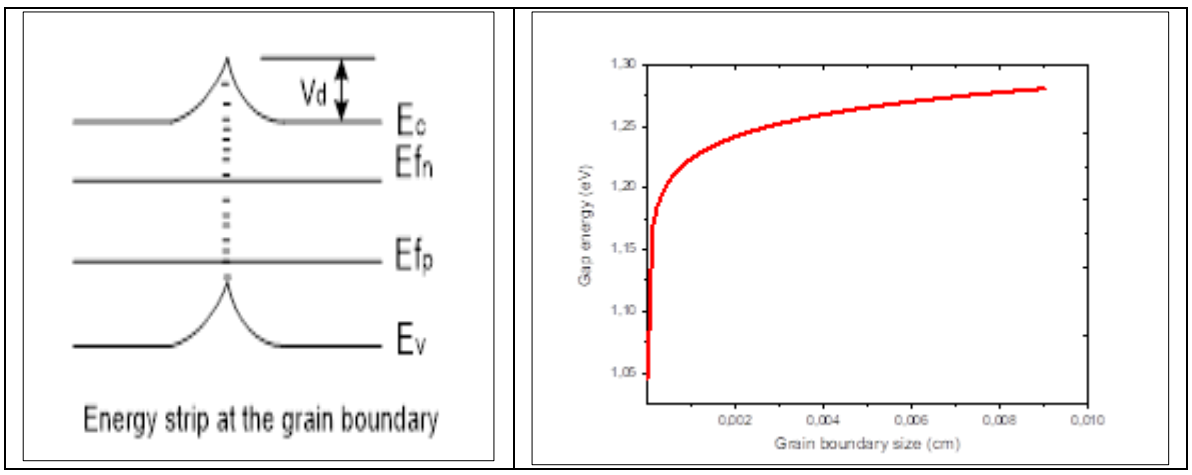

Figure 3 the evolution of the gap energy at the crystal interface in relation to the grain boundary size

The profile in Figure 3 shows the dependence of the gap energy at the crystal interface on the grain boundary size. In this figure, we see that the gap energy at the crystal interface is proportional to the grain boundary size. At the crystal surface, the electronic states are modified due to dangling bonds and layers resulting from the oxidation of silicon by oxygen. However, this modification leads to the existence of a potential barrier, which is the cause of the increase in gap energy.

2.2. Charge carrier density of the base of the bifacial solar cell

Figure 4 shows the three-dimensional figure that simultaneously illustrates the effect of depth and grain boundary size on solar cell activity under simultaneous illumination.

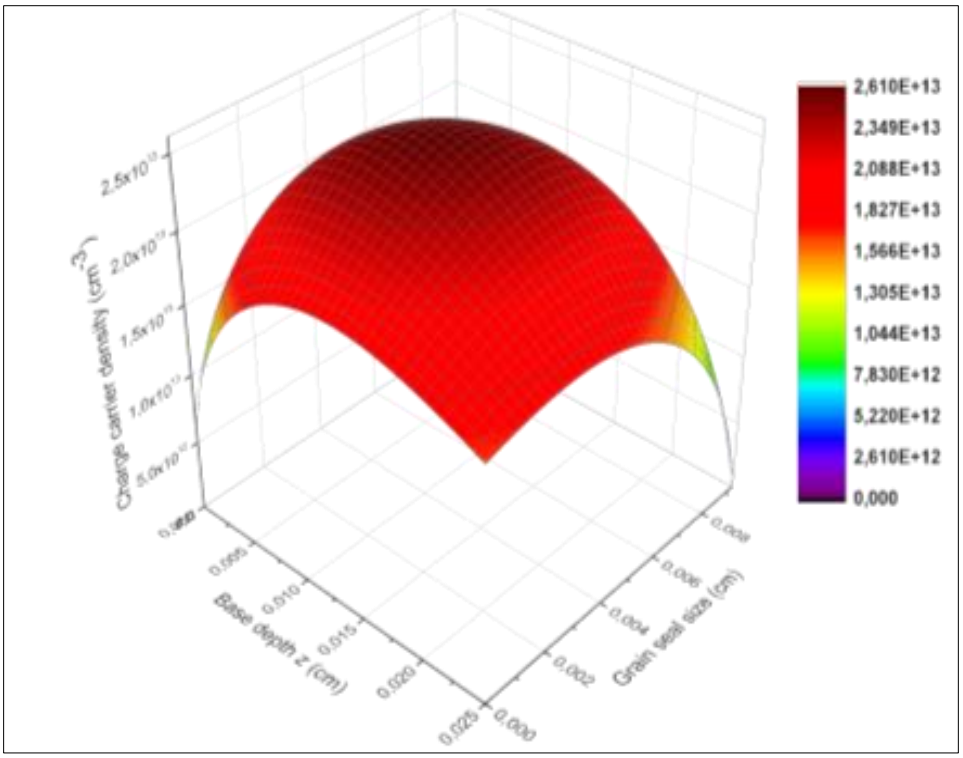

Figure 4 Effect of grain boundary depth and size on charge carrier density for simultaneous illumination

This figure shows that the depth and size of the grain boundary have a significant impact on the total photogenerated charge carrier density. Indeed, the total charge carrier density increases with depth until it reaches its maximum value, at which point it drops. This is shown in the results of [15]. However, it gradually decreases with the size of the grain boundary until it reaches its minimum value. This phenomenon shows that recombination is very active in grain boundaries, hence the reduction in carriers. The explanation is that the existence of the potential barrier in the grain boundaries tends to trap charge carriers in the grain boundaries.

Good photo-piles are obtained with a very small grain boundary size, which is accompanied by reduced boundary activity.

2.3. The current-voltage characteristic

To illustrate the influence of the shape of the grain boundary on the I-V characteristic, we felt it necessary to plot the I-V characteristic as a function of the size of the grain boundary. Figures 5 and 6 show the respective characteristics, total cell and lost in the grain boundary, when the cell is illuminated from both sides.

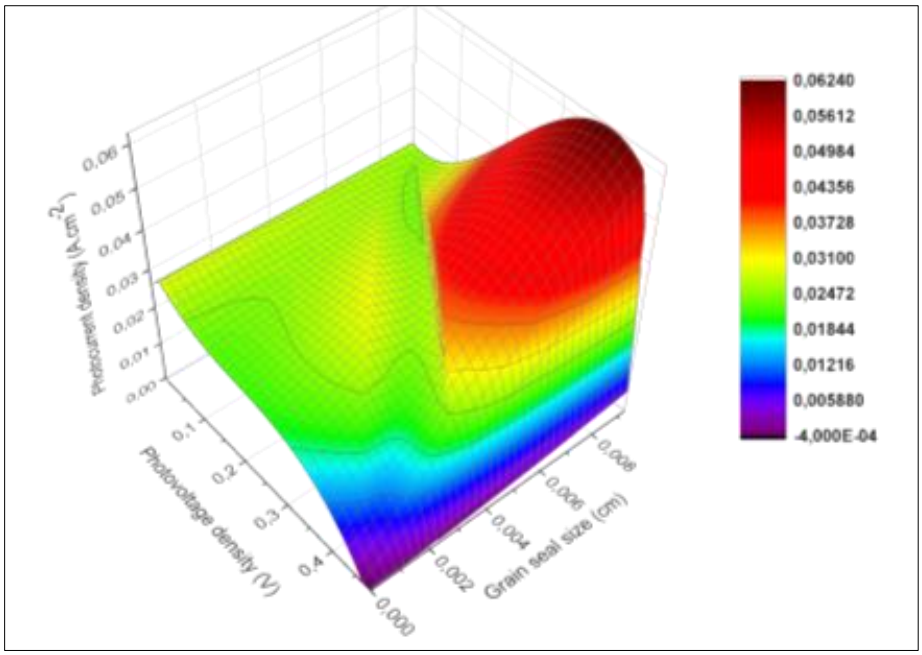

Figure 5 I-V characteristic as a function of recombination speed and grain boundary size, simultaneous illumination

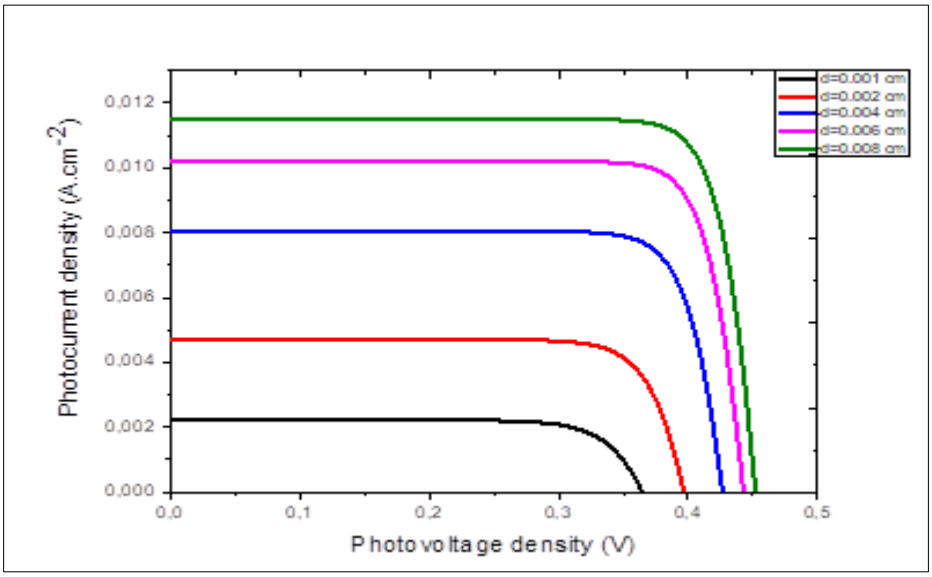

Figure 6 Current-voltage characteristics in the grain boundary for different grain boundary sizes, simultaneous illumination

The profiles in Figures 5 and 6 show that for a voltage below 0.3 V, the photocurrent density is maximum and constant, and therefore independent of the photovoltage density.

For voltage values above 0.3 V, the current density decreases rapidly to zero close to the open-circuit operating point.

The current-voltage characteristic varies between two central points [16]

- The position which characterizes the short-circuit situation where the current is maximum and the voltage almost zero ;
- The position in the open circuit situation with almost zero current and maximum voltage.

The variation of photocurrent as a function of photovoltage shows that the current-voltage characteristic evolves with the size of the grain boundary. Meanwhile, the increase in grain boundary size favours the growth of the I-V characteristic in the grain boundary. This explains the presence of charge carriers in the grain boundary as a function of its size. As a result, the carriers trapped by the existing potential barrier at the crystal interfaces are recombined. This phenomenon leads to a remarkable loss of the I-V characteristic of the solar cell.

2.4. The power delivered by the bifacial solar cell

Figures 7 and 8 show the electrical power of the photocell as a function of the recombination rate at the PN junction. However, these figures represent, respectively, the total power delivered by the photocell and that lost in the grain boundary. The cell is illuminated from both sides.

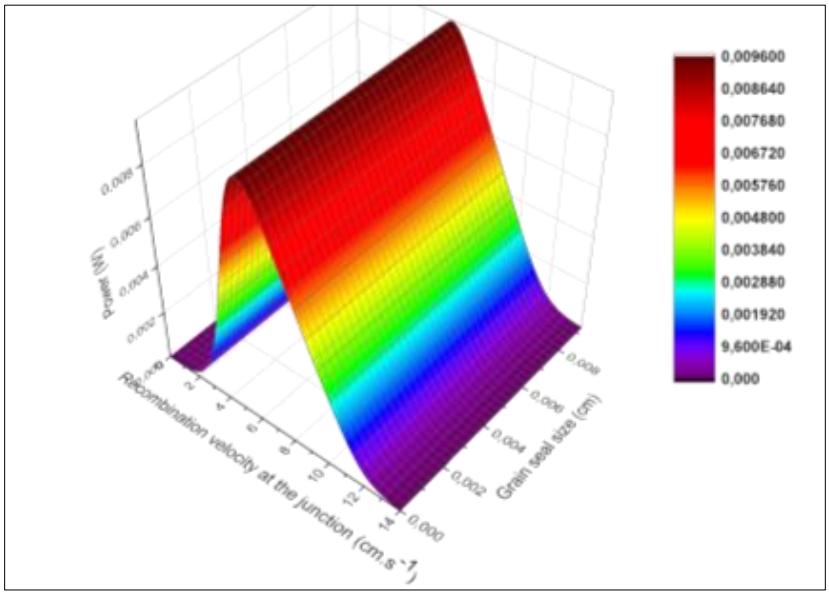

Figure 7 Photocell power as a function of recombination rate at the junction and grain boundary size, simultaneous illumination

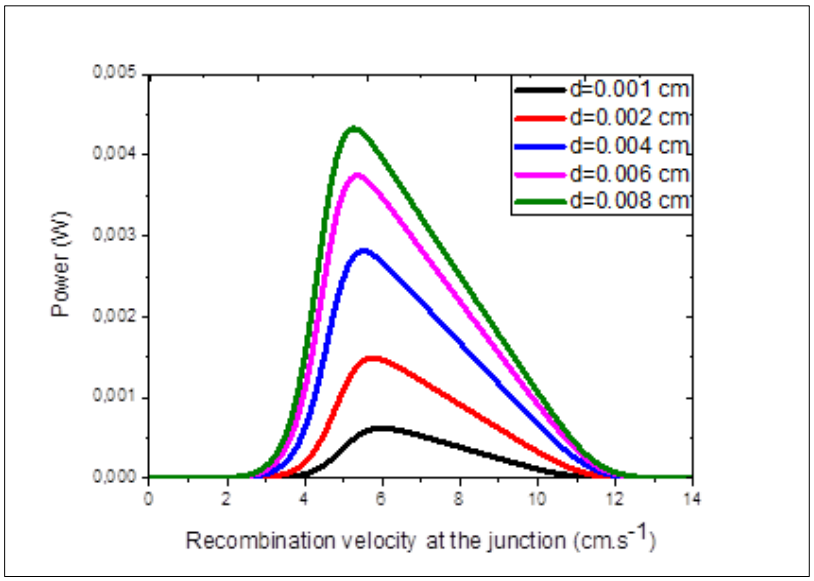

Figure 8 The power delivered by the photocell as a function of the recombination rate at the junction for different grain boundary sizes when illumination is simultaneous

Figures 7 and 8 show that, for a given bifacial cell, the power evolves as a function of the recombination rate at the PN junction. The results presented in this figure are in good agreement with those reported in the literature [17]. It also confirms their conclusion that the junction recombination rate required to obtain the maximum solar cell power point available for any grain boundary size is around $10^{5.8}$ cm.s^{-1}. These profiles also show that the grain boundary size has a very significant impact on the power generated by the cell.

Considering several identical photocells, but with increasing grain boundary sizes, we note an increase in the amplitude of the photocell power and a shift in the point of maximum power, which is accompanied by a decrease in the recombination rate at the PN junction. This is explained by the power losses of the cell due to the presence of the potential barrier at the crystal interfaces, which traps and allows the recombination of charge carriers in the grain boundary, thus reducing the performance of the solar cell.

2.5. Scattering capacity at the base-transmitter junction

Figures 9 and 10 below show the capacity of the solar cell as a function of the recombination rate at the grain boundary. These figures show, respectively, the total capacity of the solar cell and the capacity lost in the grain boundary. The solar cell is illuminated from both sides.

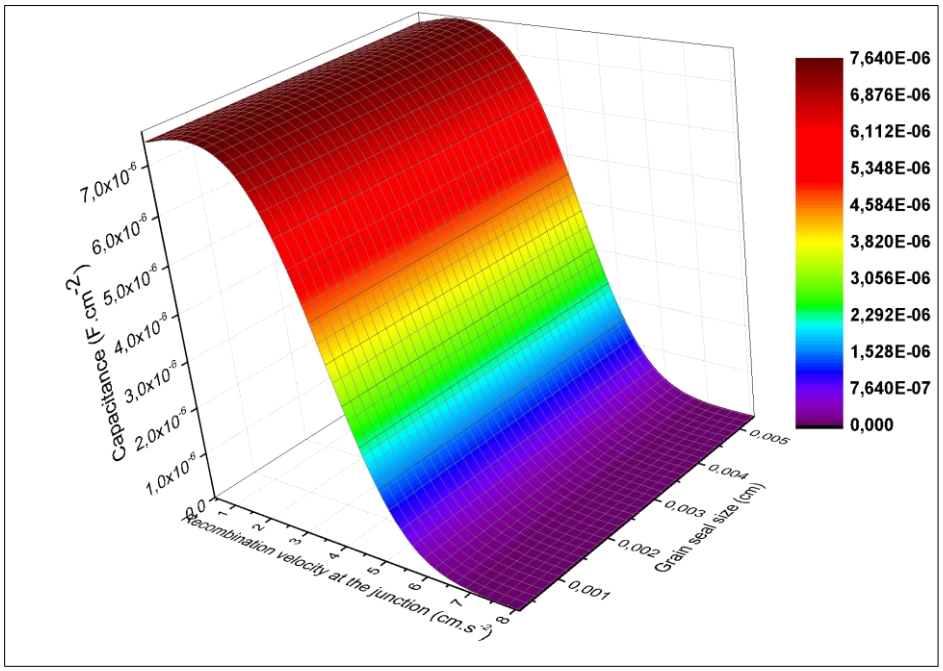

Figure 9 Photocell capacity as a function of recombination rate at the junction and grain boundary size, simultaneous illumination

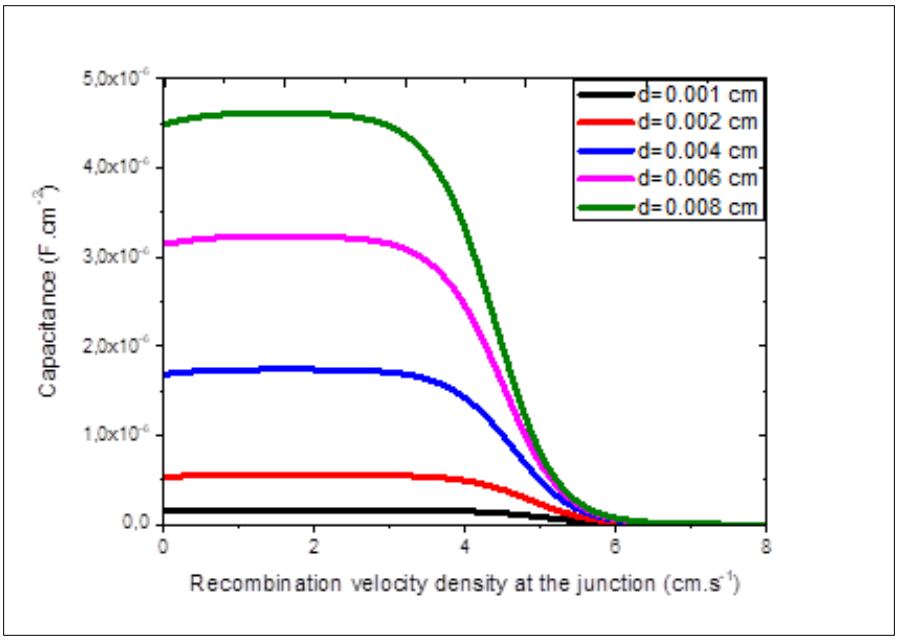

Figure 10 Cell capacity as a function of photovoltage density for different grain boundary sizes when the cell is illuminated from both sides

For figures 9 and 10, we note that the capacity of the solar cell depends on the recombination rate at the junction and the shape of the grain boundary [14].

When excess minority carriers diffuse into the base of a solar cell, part of the carriers cross the base-emitter junction. The remaining part induces the cell's diffusion capacity. This comes from the transport of excess minority carriers into the base of the solar cell.

Figure 9 shows that the diffusion capacity decreases with the rate of recombination at the junction. Near the open circuit, all of the excess minority carriers are stored in the cell, resulting in a higher capacity. The diffusion capacity decreases with higher values of the recombination rate at the junction. This is due to the large flow of carriers through the junction, which consequently reduces their storage in the cell.

In Figure 10, the increase in grain boundary size favours the growth of the diffusion capacity in the grain boundary. This reflects the losses of charge carriers leading to a reduction in the cell's diffusion capacity.

2.6. Study of production losses in a solar cell made up of cylindrical grains

Table 1 Variation in the electrical parameters of two grains and the grain boundary of the multi-cylinder grain solar cell.

Electrical parameters	Total production for two cylindrical grains	Electrical parameters in the grain boundary (losses)
δ ($10^{13}cm^{-3}$)	4.04	0.84
P ($mA.cm^{-2}$)	0.0236	0.0044
C ($10^{-6}F.cm^{-2}$)	17.34	4.5

The table shows the charge carrier density of a bifacial solar cell illuminated from both sides, the power delivered by the cell and the diffusion capacity at the base-emitter junction of the grains and the grain boundary of a multi-cylinder grain solar cell. However, we found a very significant production loss rate. This reduction is 20.79 % for the charge carrier density, 18.64 % for the power and 25.95 % for the capacity of the solar cell.

Numerical analysis is a calculation method that can be used to solve any given problem, leading to a single, precise result. This is how numerical analysis distinguishes itself from other, more traditional mathematical methods of solving problems, such as the separation of variables method. In fact, for a given problem, it is possible to use several numerical resolution methods, resulting in different algorithms. These depend on certain parameters that influence the accuracy of the result.

The final result and its degree of accuracy depend on the choices made. An important part of numerical analysis is therefore to contain the effects of the errors thus introduced, which come from three main sources:

- Modeling errors ;
- Computer representation errors;
- Truncation errors.

$$\text{relative error} = \frac{\left|\delta - \delta^*\right|}{\left|\delta\right|} = 9.99 \cdot 10^{-4}$$

3. Conclusion

In this study, a method for specifying the equivalent electrical parameters associated with the shape of the grain boundaries in a bifacial photovoltaic solar cell composed of cylindrical grains was presented. The solar cell is subjected to a static regime and illuminated simultaneously from both sides. The results show that the shape of the grain boundaries has a negative effect on the production activity of the multicylindrical grain solar cell. The results show very significant losses due to the trapping and recombination of charge carriers in the grain boundaries. For production, we note a loss rate of 20.79% for the charge carrier density, 18.64% for the power delivered by the solar cell and 25.95% for the diffusion capacity.

The aim of this work was to investigate some possible improvements in the I-V characteristic, power and diffusivity of the solar cell. These improvements may come from a reduction in recombination at the grain boundaries. Experimentally, this parameter can be controlled by passivation the recombination site.

Compliance with ethical standards

Disclosure of conflict of interest

No conflict of interest to be disclosed.

References

[1] D. R. Clarke et D. Wolf, « Chapter 3 grain boundaries in ceramics and at ceramic-metal interfaces », Mater. Sci. Eng., vol. 83, no 2, p. 197-204, nov. 1986.

[2] J. Oualid, C. M. Singal, J. Dugas, J. P. Crest, et H. Amzil, « Influence of illumination on the grain boundary recombination velocity in silicon », J. Appl. Phys., vol. 55, no 4, p. 1195-1205, févr. 1984.

[3] N. Bernstein, « The influence of geometry on grain boundary motion and rotation », Acta Mater., vol. 56, no 5, p. 1106-1113, mars 2008.

[4] T. Saga, « Advances in crystalline silicon solar cell technology for industrial mass production », NPG Asia Mater., vol. 2, no 3, p. 96-102, juill. 2010.

[5] S. Pouladi et al., « Effects of grain boundaries on conversion efficiencies of single-crystal-like GaAs thin-film solar cells on flexible metal tapes », Sol. Energy Mater. Sol. Cells, vol. 199, p. 122-128, sept. 2019.

[6] H. C. Card et E. S. Yang, « Electronic processes at grain boundaries in polycrystalline semiconductors under optical illumination », IEEE Trans. Electron Devices, vol. 24, no 4, p. 397-402, avr. 1977.

[7] M. Imaizumi, T. Ito, M. Yamaguchi, et K. Kaneko, « Effect of grain size and dislocation density on the performance of thin film polycrystalline silicon solar cells », J. Appl. Phys., vol. 81, no 11, p. 7635-7640, june 1997.

[8] A. Castro-Méndez, J. Hidalgo, et J. Correa-Baena, « The Role of Grain Boundaries in Perovskite Solar Cells », Adv. Energy Mater., vol. 9, no 38, p. 190-1489, Oct. 2019.

[9] L. L. Kazmerski, « The effects of grain boundary and interface recombination on the performance of thin-film solar cells », Solid-State Electron., vol. 21, no 11-12, p. 1545-1550, nov. 1978.

[10] M. L. Samb, M. Zoungrana, F. Toure, M. T. D. Diop, et G. Sissoko, « étude en modelisation a 3-d d'une photopile au silicium en regime statique placee dans un champ magnetique et sous éclairement multispectral : determination des parametres electriques », J. Sci., vol. 10, 2010.

[11] A. Diouf, S. N. Leye, S. Mbodji, A. Diao, et G. Sissoko, « 3d cylindrical approach to determine the excess minority carriers' density of an n+/p solar cell under constant monochromatic illumination », 33rd Eur. Photovolt. Sol. Energy Conf. Exhib.

[12] A. Trabelsi, A. Zouari, et A. B. Arab, « Modeling of polycrystalline N+/P junction solar cell with columnar cylindrical grain », Rev. Energ. Renouvelables, vol. 12, no 2, p. 279-297, 2009.

[13] M. S. Diouf, G. Sahin, A. Thiam, K. Faye, et M. I. Ngom, « Determination Of The Junction Surface recombination Velocity Limiting The Open Circuit (Sfoc) For A Bifacial Silicon Solar Cell Under External Electric Field. », IJISET - Int. J. Innov. Sci. Eng. Technol., vol. 2, no 9, p. ISSN 2348-7968, sept. 2015.

[14] S. Mbodji, M. Dieng, B. Mbow, F. Barro, et G. Sissoko, « Influence of grain size and grain boundary recombination velocity on the diffusion capacitance of a polycrystalline bifacial silicon solar cell », J. Sci. Pour Ing., vol. 11, no 1, juill. 2011.

[15] S. Mbodji, B. Mbow, F. I. Barro, et G. Sissoko, « A 3D model for thickness and diffusion capacitance of emitter-base junction determination in a bifacial polycrystalline solar cell under real operating condition », Turk. J. Phys., janv. 2011.

[16] S. Madougou, F. Made, M. S. Boukary, et G. Sissoko, « I –V Characteristics For Bifacial Silicon Solar Cell Studied Under a Magnetic Field. », Adv. Mater. Syst. Technol., vol. 18-19, p. 303-312, 2007.

[17] A. G. Camara et al., « Determination of the Shunt and Series Resistances of a Vertical Multijunction Solar Cell under Constant Multispectral Light », 26th Eur. Photovolt. Sol. Energy Conf. Exhib.